

## Motivation

Equatorial plasma bubbles (EPBs) are regions of the ionosphere with irregular densities and sharp density gradients between the bubble and surrounding plasma which form in the lower geomagnetic latitudes in the upper thermosphere/ionosphere region (F4). These EPBs form in the post-sunset region of the ionosphere and have a distinct optical signature (Eastes et al., 2017). The density gradients are often more than two orders of magnitude lower than the relative background plasma density (Magdalena et al., 2016). These irregular density gradients and small-scale structures that form along the EPBs can interfere with over-the-horizon radar and GPS, respectively. This is cause for interest to researchers and those in industry alike (Eastes et al., 2017; Magdalena et al., 2016). The preprocessing of data also becomes a major bottleneck as a given dataset gets larger. A preliminary look at the potential uses of machine learning (ML) for object classification (OC) is also discussed to address this.

## Automated Detection and Tracking

The automated EPB detection and tracking algorithm presented provides a method of processing GOLD data for the detection of EPBs with subsequent tracking and analysis of EPBs. This is implemented on 4 years of GOLD data to develop a large database of EPB detections that can be used to generate useful statistics on the nature of EPBs.

- Temporal cadence has varied throughout the GOLD mission with special operations and changing mission parameters. The method has been designed to operate with this varied frequency of data.
- While GOLD data is the focus, the method has been designed so that some, or all, of the process can be applied to other data sets.

## GOLD Mission and Data Used

- Geostationary orbit at 0° latitude and -47.5° longitude.
  - Continues spatial and temporal data of the Earth limb and disk.
    - 132nm - 162nm emissions observed.
    - Temperature and composition can be gleaned from these measurements.
  - Nightside data used for this study looks at 135.6 nm emissions.
    - Recombination of O<sup>+</sup> with electrons.
    - Alternating north and south scans taken ~15min intervals.
    - Simultaneous north and south scans later in the evening.
    - Focus on low latitudes.
    - Start east along the limb and follow the dayside terminator west.
    - Pixel resolution of ~ 95-95 km at NADIR.
  - Date range for this study: October 5, 2018 to September 30, 2022.
    - Nightside Version 4 data is used.
- (Eastes et al., 2017, 2019, 2020; McClintock et al., 2020).

## Data Preprocessing

1. Cubic spline interpolation is implemented in data array space to increase density of data (figures 1a and 2b).
2. Nearest neighbor interpolation (NN) is implemented on individual scans after cubic spline interpolation.
  - NN grids are 0.5 x 0.5 degrees centered at every half degree north and south and east to west (figure 1a).
  - Note the regions of the NN grid that would be devoid of data for a traditional NN algorithm in figure 1b.
  - High latitudes are removed during this step to improve processing times.

## Nearest Neighbor Regions

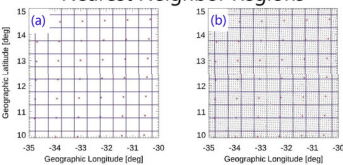


Figure 1. Zoomed in northern GOLD data scan from November 28, 2018 at 2310 UTC. Data's geographic locations of the cube are visible in figure (a) in red, while figure (b) shows the implementation of the cubic spline interpolation overlaid in black. Figures (a) and (b) both show NN grid lines overlaid in blue.

## References

Eastes, R. W., McClintock, W. E., Burns, A. G., Anderson, D. N., Anderson, L., Codrescu, M., ... Oberheide, J. (2017). The global-scale observations of the limb and disk (gold) mission. *Space Science Reviews*, 212, 383-408. doi: 10.1007/s11214-017-0392-2

Eastes, R. W., Solomon, S. C., Daniell, R. W., Anderson, D. N., Burns, A. G., England, S. L., ... McClintock, W. E. (2019). Global-scale observations of the equatorial ionization anomaly. *Geophysical Research Letters*, 46, 9318-9326. doi: 10.1029/2019GL084199

Eastes, R. W., McClintock, W. E., Burns, A. G., Anderson, D. N., Anderson, L., Aryal, S., ... Woods, T. N. (2020). Initial observations by the gold mission. *Journal of Geophysical Research: Space Physics*, 125, e2020JA027823. doi: 10.1029/2020JA027823

Magdalena S., Herranz M., Akhalidi D., Moreira B.A. Climatology characterization of equatorial plasma bubbles using GPS data. *Journal of Space Weather and Space Climate*, 7, A3. https://doi.org/10.1051/swsc/2016039

McClintock, W. E., Eastes, R. W., Hockins, A. C., Siegmund, O. H. W., McPhate, J. B., Krywonus, A., ... Burns, A. G. (2020). Global-scale observations of the limb and disk mission implementation: 1. Instrument design and early flight performance. *Journal of Geophysical Research: Space Physics*, 125, doi: 10.1029/2020JA027797

Prahdita, R., Valladares, C. E., & Doberty, P. H. (2015). An effective ice data detrending method for the study of equatorial plasma bubbles and traveling ionospheric disturbances. *Journal of Geophysical Research Space Physics*, 120, 11048-11055. doi: 10.1002/2015JA021723

## Data Pairing

1. Preprocessed north and south scans are combined to form images (figure 1a).
2. Data are converted onto a regular grid in Quasi-Dipole (QD) coordinates to identify and later track features about the magnetic equator (figure 2b).
3. QD latitude and solar zenith angle cutoffs are implemented to prevent polar and solar influence (figure 2b).

## NN Data Pair and QD Conversion

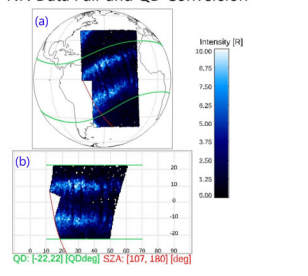


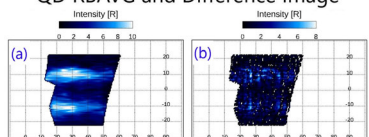
Figure 2. Preprocessed GOLD data scans from the night of November 28, 2018 at 2310 UTC. Paired GOLD data scans from a full north and south image with high latitudes removed (a). Data from (a) converted to QD coordinates with QD and SZA cutoffs implemented (b). QD and SZA cutoffs are overlaid in green and red, respectively.

## Crest Detection and Detrending

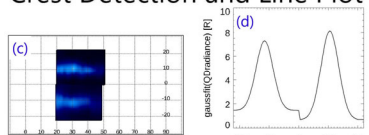
Detrending and EIA crest detection are implemented to pick out EPBs within images. Detrending is done with the use of a rolling barrel average (RBVAG); developed by Prahdita et al. (2015).

1. RBVAG is computed along QD latitudes (figure 3a).
  - RBVAG simulates a 'barrel' rolling over data for detrending.
2. Difference images computed: RBVAG minus QD data (figure 3b).
3. A running average and Gaussian fit are computed across the northern and southern magnetic regions independently (figure 3c).
  - A peak value in the magnetic north and magnetic south can then be selected as the crest of the northern and southern EIA regions (figure 3d).
4. The EIA crests are used to define an EPB summation region, later used for summations along QD longitudes (figure 3e).

## QD RBVAG and Difference Image



## Crest Detection and Line Plot



## QD Difference Summation Regions

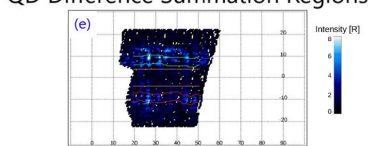


Figure 3. RBVAG implemented on QD data from figure 2b (a), difference image computed from RBVAG minus QD data (b), running average and Gaussian fit across both QD northern and southern regions (c), plot along QD longitude of 30 QDdegrees (d), summation regions along the northern EIA, QD equator, and southern EIA demarcated by green, orange, and red curves, respectively, used for EPB detection. The topmost green curve is the detected northern EIA crest, and the bottommost red curve is the detected southern EIA crest (e). All in QD coordinates.

## EPB Detection

1. Summations are computed along lines of QD longitude within each detection region of the difference data. Peaks along these summations correlate with EPB detections along the EIA crests and the magnetic equator.
    - An example of this is provided in figure 4a.
    - The black curve is the summation of the southern detection region used to pick out potential EPBs. Black and red stars mark potential EPBs.
  2. Uncertainties, shown as blue vertical bars, are used to compare peaks with neighboring valleys to remove false positives.
    - If peak minus uncertainty is less than both neighboring valleys plus their respective uncertainties, then then peak is deemed false and removed.
    - Peaks that are kept are shown in red, and those that are removed in black (figure 4a).
- Detections kept for analysis are shown in figures 4b and 4c in red.

Figure 4. EPB detection from the night of November 28, 2018 at 2310 UTC. Summation of southern EIA's detection region with uncertainties shown as vertical blue bars, removed EPB detections marked in black, kept EPB detections marked in red (a). Final EPB detections in geographic and QD coordinates are shown in figures (b) and (c), respectively, in red.

## Analysis

Images generated and their EPB detections can be used to calculate drift speeds by comparing subsequent images in time. Figure 5 shows an example of EPBs from subsequent images being compared. EPB detections in figure 5a (marked in red) are compared with EPB detections in figure 5c (marked in green) with 5a's EPBs overlaid. Figure 5a is then checked with figure 5b as they both have a common scan.

Figure 5c is then compared with a valid image to compare with 5a.

If the starting image were instead 5b, then 5d would be used.

EPB detections that are used to calculate a drift speed are given a unique count value (1, 2, 3, etc...) to track EPBs as they drift.

- Those that are not tracked are removed from the database, as these are most often false positives.

Figure 5. EPB images in QD coordinates from the night of November 28, 2018 in order: (a), (b), (c), and (d). UT and geographic region ('N' for north and 'S' for south) of each scan is labeled at the top of each plot. For example, the image in (b) is made from geographic scans in the south and north taken at 2310 UTC and 2325 UTC, respectively.

## Statistics

Figures 6a and 6b show the drift speeds along the northern EIA and southern EIA, respectively, as a percent of total EPBs split by season: December solstice (Nov - Feb), March equinox (March - April), June solstice (May - August), and September equinox (September - October). The top right of each plot contains the legend for seasons and the total EPBs detected for the region and season.

- Seasonality is evident with the majority of EPBs occurring during the December solstice and fewer occurring during the June solstice.
  - This is corroborated with time series of plots from 2018 to 2022 of EPBs (not displayed).
- Distributions are largely similar across regions and seasons.
- Means (dotted lines) and medians (dashed lines) are similar across regions and seasons.
- While not displayed here, the same is true of measures of width and EPB bubble separations.

Figure 6. Drift speed histograms of all data analyzed from October 5, 2018 to September 30, 2022. Figures (a) and (b) show EPB drift speeds along the northern EIA and southern EIA, respectively. Horizontal axis is drift speed in [m/s] with bin size of 20 [m/s]. The vertical axis is percent of total for each region and season. The top right of each plot serves as the season legend and shows the total EPB count for that region and season. Means are displayed as dotted vertical lines while medians are dashed.

## Machine Learning for Classifying EPBs

The most time and computationally expensive elements of this process are the preprocessing of data onto a usable regular QD grid and the conversion of EPB detections from QD to geographic coordinates. The use of ML algorithms for OC can potentially eliminate the need for exhaustive preprocessing of data and the conversion from geographic, to QD, and back to geographic. To see if this is feasible, an initial check using the You Only Look Once version 4 (YOLOv4) convolution neural network for OC is implemented.

## Training and Testing

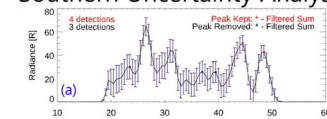
1. 80% of the entire database is used to train YOLOv4.
2. QD heat maps and coordinates are used for this first run.
3. The remaining 20% is used to test and verify proper classifications.

## Test Output

A test output of EPBs classified by YOLOv4 is provided in figure 7.

- Northern EIA EPBs (green boxes).
- Magnetic equator EPBs (purple boxes).
- Southern EIA EPBs (red boxes).
- Confidence of classifications vary from 46% to 98% confidence.
  - Higher confidence generally correlates with larger gradient in radiance between EPB and surrounding plasma.
- EPB around 32 QD degrees longitude in the north and south are not classified
- 2 EPBs around 28 and 32 QD degrees longitude are classified as a single EPB along the magnetic equator.

## Southern Uncertainty Analysis



## Final Image Used for Detection

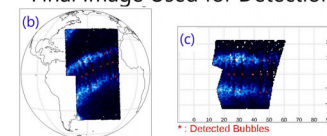
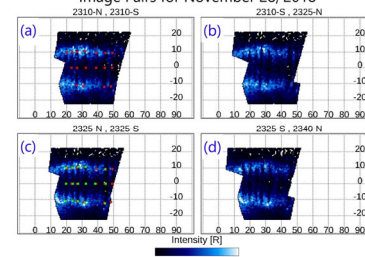
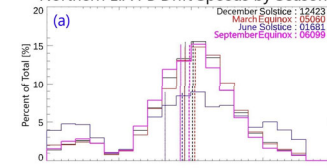


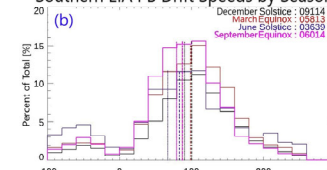
## Image Pairs for November 28, 2018



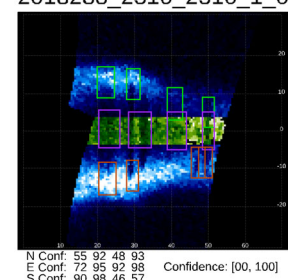
## Northern EIA PB Drift Speeds by Season



## Southern EIA PB Drift Speeds by Season



## 2018288 2310 2310\_1\_0



## Reference and Source Code

• Reference: <https://arxiv.org/abs/2004.10934v1>

• Source code: <https://github.com/AlexeyAB/darknet>